# Characterization of Human Angiogenin Variants Implicated in Amyotrophic Lateral Sclerosis†

Benedict Crabtree,‡ Nethaji Thiyagarajan,‡ Stephen H. Prior,‡,§ Peter Wilson,‡ Shalini Iyer,‡ Tyrone Ferns,|| Robert Shapiro,⊥ Keith Brew,|| Vasanta Subramanian,*,‡ and K. Ravi Acharya*,‡

*Department of Biology and Biochemistry, University of Bath, Claverton Down, Bath BA2 7AY, United Kingdom, College of Biomedical Science, Florida Atlantic University, 777 Glades Road, Boca Raton, Florida 33431, and Department of Pathology, Center for Biochemical & Biophysical Sciences & Medicine, Harvard Medical School, Boston, Massachusetts 02115*

*Received July 6, 2007; Revised Manuscript Received August 8, 2007*

ABSTRACT: Human angiogenin (ANG), the first member of the angiogenin family (from the pancreatic ribonuclease A superfamily) to be identified, is an angiogenic factor that induces neovascularization. It has received much attention due to its involvement in the growth of tumors and its elevated expression level in pancreatic and several other cancers. Recently the biological role of ANG has been shown to extend to the nervous system. Mutations in *ANG* have been linked with familial as well as sporadic forms of amyotrophic lateral sclerosis (ALS), a fatal neurodegenerative disorder characterized by selective destruction of motor neurons. Furthermore, mouse angiogenin-1 has been shown to be expressed in the developing nervous system and during the neuronal differentiation of pluripotent stem cells. We have now characterized the seven variants of ANG reported in ALS patients with respect to the known biochemical properties of ANG and further studied the biological properties of three of these variants. Our results show that the ribonucleolytic activity of six of the seven ANG-ALS implicated variants is significantly reduced or lost and some variants also show altered thermal stability. We report a significant reduction in the cell proliferative and angiogenic activities of the three variants that we chose to investigate further. Our studies on the biochemical and structural features of these ANG variants now form the basis for further investigations to determine their role(s) in ALS.

Amyotrophic lateral sclerosis (ALS)[1] is a fatal neurodegenerative disorder characterized by selective destruction of motor neurons (*1*). In the past decade, a small number of genes involved in the etiology of the disease have been identified (for a recent review see ref *2*). The best studied of these is *SOD1* (*3*), the gene for Cu/Zn superoxide dismutase. More than a hundred *SOD1* mutations have now been linked with ALS, and motor neuron death from many of these mutations has been shown to result from a toxic gain of function rather than loss of dismutase activity. However, mutations in *SOD1* account for only 1−2% of all cases of ALS and 20% of the familial cases. Some of the other proteins implicated in ALS are the vesicle-trafficking protein VAPB (*4*); ALSIN, a putative guanine nucleotide factor for GTPase (*5*); and senataxin (*6*). In addition, vascular endothelial growth factor (VEGF), an angiogenic factor that plays an important role in motor neuron survival, has been linked with ALS (*7*−*10*). However, the causes and molecular mechanisms underlying ALS are still largely unclear, and effective therapies do not appear to be imminent.

Angiogenin (*ANG*), which encodes an angiogenic protein, was recently identified as a candidate susceptibility gene for ALS in the Irish and Scottish population by Greenway et al. (*11*). In a further study of over 2500 individuals from five independent populations from northern Europe and North America, Greenway et al. (*12*) found seven missense mutations (Figure 1) in 11 unrelated individuals with sporadic ALS and in four individuals with familial ALS. Mutations were identified in five different populations, although 12 of the 15 individuals with *ANG* mutations were of Irish or Scottish descent. Mutations segregated with the disease and not with unaffected family members or >2000 ethnically matched control chromosomes. Moreover, ANG was shown to be expressed in mouse spinal cord motor neurons. These findings suggest that *ANG* mutations cause both familial and sporadic ALS and that ANG has an important function in the nervous system. In a recent report, Subramanian and Feng (*13*) have shown that ANG is expressed strongly in the developing nervous system in the mouse and during neuronal differentiation of pluripotent stems cells, suggesting a role for this protein in neurite pathfinding.

† This work is supported by the Wellcome Trust (U.K.) through a Programme Grant (083191) to K.R.A. and a postgraduate studentship to B.C. (073153) under the joint supervision of V.S. and K.R.A.

* To whom correspondence should be addressed: (K.R.A.) phone +44-1225-386238, fax +44-1225-386779, e-mail bsskra@bath.ac.uk; (V.S.) phone +44-1225-386315, fax +44-1225-386779, e-mail bssvss@bath.ac.uk.

‡ University of Bath.

§ Present address: Cancer Sciences Division, Southampton General Hospital, Tremona Road, Southampton SO16 6YD, U.K.

|| Florida Atlantic University.

⊥ Harvard Medical School.

[1] Abbreviations: ALS, amyotrophic lateral sclerosis; ANG, angiogenin; BSA, bovine serum albumin; CD, circular dichroism; ESMS, electrospray ionization mass spectrometry; FCS, fetal calf serum; GFR, growth factor-reduced; MS, mouse serum; MTT, 3-(4,5-dimethylthiazol-2-yl)-2,5-diphenyltetrazolium bromide; PBS, phosphate-buffered saline; RNase A, ribonuclease A; SOD, superoxide dismutase.

10.1021/bi701333h CCC: $37.00 © 2007 American Chemical Society
Published on Web 09/27/2007

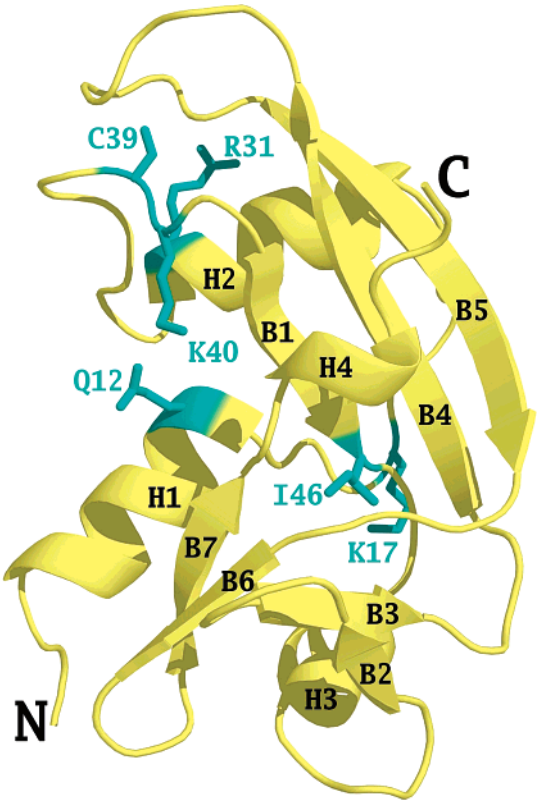


FIGURE 1: Structural overview highlighting the location of mutations. A ribbon diagram of the ANG structure (colored pale yellow) with mutation sites implicated in ALS is shown. The N- and C-termini and elements of secondary structure (H, helix; B, $\beta$-strand) are labeled. Mutated residues (drawn in stick form) are shown in cyan and are labeled. Figure was created with the program PyMOL (http://www.delanoscientific.com).

Human ANG, a 14.1 kDa protein, is a potent inducer of neovascularization in vivo (*14*) with a sequence that is 33% identical to that of bovine RNase A (for reviews see refs *15* and *16*). Its enzymatic activity toward conventional RNase substrates is several orders of magnitude lower than that of RNase A (*17*, *18*) but is important for its biological activity. ANG mutants with decreased enzymatic activity invariably have reduced angiogenic activity (*19*−*22*).

The detailed mechanism of action of ANG has yet to be clearly established. However, it has been shown that accumulation of ANG in the nucleolus of target endothelial cells is essential for its biological activity (*23*, *24*) and that ANG binds to a receptor on the surface of endothelial cells (*25*, *26*) and induces a variety of activities required for angiogenesis (*26*−*28*). ANG has been shown to be upregulated by hypoxia in cultured melanoma cells (*29*) and in human renal proximal tubular epithelial cells (*30*).

At the molecular level, crystal structures of ANG [human angiogenin (Figure 1) (*31*, *32*), bovine angiogenin (*33*), and murine angiogenins −1 (*34*) and −4 (*22*)] have revealed the RNase A fold and conservation of the catalytic triad His13, Lys40, and His114 (ANG numbering). These structures, together with extensive functional and biochemical data, have provided a detailed understanding of the architecture of the ANG active site and the roles of the various residues involved in the binding and cleaving of RNA.

In order to understand the properties of the ANG-ALS variants, we constructed and expressed these variants and determined their thermal stability and ribonucleolytic activity. In addition, we have characterized the effects of three of these mutations that markedly reduce ribonucleolytic activity (Q12L, C39W and K40I) on the established angiogenic and mitogenic properties of ANG. In parallel, the effects of these three ANG variants on neurons and their survival were studied and will be reported elsewhere (Subramanian et al., unpublished results).

## EXPERIMENTAL PROCEDURES

*Protein Engineering, Expression, and Purification of Variants.* A synthetic gene for wild-type ANG with *Escherichia coli* codon bias (*35*) was inserted into pET-22b(+) (Novagen) for expression of the Met-(−1) form of the protein (*34*). The Stratagene QuikChange site-directed mutagenesis kit was used to introduce mutations with the oligonucleotides listed in Table 1. After DNA sequencing (MWG, Germany) to confirm the presence of the mutations and the absence of any unintended changes, mutant plasmids were used to transform *E. coli* BL21(DE3) cells. Recombinant proteins were prepared from these strains by the method of Holloway et al. (*36*). Briefly, the bacterial cells were grown in Terrific broth at 37 °C to an $OD_{600}$ of 0.5−0.6, after which expression was induced by addition of IPTG to a final concentration of 1 mM and incubation was continued for ∼3 h before harvesting. The target proteins were deposited as inclusion bodies. These were extracted, refolded, and purified by SP-Sepharose chromatography followed by C4 reversed-phase HPLC. Purified proteins were lyophilized and dissolved in AnalaR grade water. All ANG variants behaved similarly to the wild-type protein during purification. Concentrations of recombinant proteins were determined from UV absorbance, with an $\epsilon_{280}$ value of 12 500 $M^{-1}$ $cm^{-1}$ for wild-type ANG (*37*) and all variants except for C39W; an $\epsilon_{280}$ value of 17 875 $M^{-1}$ $cm^{-1}$, calculated by the method of Pace et al. (*38*), was used for C39W.

The purity of each protein was >98%, as judged by SDS−PAGE and analytical scale reverse-phase HPLC. Protein molecular masses were determined by electrospray ionization mass spectrometry (ESMS). Protein solutions were prepared for mass spectrometry by dilution of a desalted standard stock solution of protein in water (1 mg/mL, ≈70 $\mu$M) in a 50:50 ratio with HPLC-grade acetonitrile containing 0.1% formic acid. ESMS was performed in positive ion mode on a QStar XL System (Applied Biosystems), fitted with a NanoMate (Advion Biosciences) automated nanospray source. A delivery pressure of 0.3 psi of nitrogen gas and a spray voltage of 1.6 kV were applied to the sample to generate the nanospray plume. Transformed mass spectra were calculated by use of the Bayesian protein reconstruct algorithm provided as part of the MDS Sciex Analyst 1.1 software package. Molecular mass measurements were in agreement with the masses predicted for the Met-(−1) form of each protein, except for the C39W variant, whose mass was 306 units greater than expected; the increased mass for C39W most likely reflects the attachment of a glutathione molecule to Cys92, which is normally disulfide-bonded to Cys39.

*Ribonucleolytic Activity Assay.* Activity toward tRNA was determined by measuring the formation of acid-soluble fragments as described by Shapiro et al. (*39*). Assay mixtures contained 2 mg $mL^{-1}$ yeast tRNA (Sigma), 0.1 mg $mL^{-1}$

Table 1: Oligonucleotide Primers Used for the Generation of ANG Variants

| mutation | | primers (5′ → 3′) |
|---|---|---|
| Q12L | sense | GTATACACATTTCCTGACC**CTG**CACTATGACGCTAAACCG |
| | antisense | CGGTTTAGCGTCATAGTG**CAG**GGTCAGGAAATGTGTATAC |
| K17I | sense | CACTATGACGCT**ATA**CCGCAGGGCCG |
| | antisense | CGGCCCTGCGG**TAT**AGCGTCATAGTG |
| K17E | sense | CACTATGACGCT**GAA**CCGCAGGGCC |
| | antisense | GGCCCTGCGG**TTC**AGCGTCATAGTG |
| R31K | sense | CGAATCGATTATG**AAA**CGCCGTGGGTTAAC |
| | antisense | GTTAACCCACGGCG**TTT**CATAATCGATTCG |
| C39W | sense | GGGTTAACTAGTCCG**TGG**AAAGATATCAACACTTTC |
| | antisense | GAAAGTGTTGATATCTTT**CCA**CGGACTAGTTAACCC |
| K40I | sense | GGGTTAACTAGTCCGTGC**ATC**GATATCAACACTTTCATCC |
| | antisense | GGATGAAAGTGTTGATATC**GAT**GCACGGACTAGTTAACCC |
| I46V | sense | GATATCAACACTTTC**GTC**CATGGTAACAAGCG |
| | antisense | CGCTTGTTACCATG**GAC**GAAAGTGTTGATATC |

bovine serum albumin (BSA), and 0.05, 0.1, 0.2, 0.3, 0.4, or 0.5 $\mu$M test protein in 33 mM Na-Hepes and 33 mM NaCl, pH 7.0. After 2 h of incubation at 37 °C, reactions were terminated by the addition of 2.3 volumes of ice-cold 3.4% perchloric acid. The mixtures were then centrifuged at 13000*g* for 10 min at 4 °C, and the absorbances of the supernatants were measured at 260 nm.

*Cell Proliferation Assays.* The effects of wild-type ANG and selected variants on the proliferation of IGR1 melanoma cells were studied as described previously by Crabtree et al. (*22*). Cells were seeded in 48-well tissue culture plates (Falcon-BD) at a density of $5 \times 10^3$ cells well$^{-1}$ in Earle's minimal essential medium supplemented with 10% FCS, 2 mM L-glutamine, and 25 mM $NaHCO_3$. After 24 h of culture to allow cell attachment, the monolayer was washed three times with phosphate-buffered saline (PBS), and low-serum medium (same as above but with 0.1% FCS) supplemented with 200 ng mL$^{-1}$ ANG or ANG variant was added. Cells treated with low-serum medium alone were used as a negative control. Incubations were carried out at 37 °C, under 5% $CO_2$. Cell proliferation was measured at 24-h intervals over 4 days by use of a 3-(4,5-dimethylthiazol-2-yl)-2,5-diphenyltetrazolium bromide (MTT) cell proliferation kit (Promega). All data were analyzed by Student's paired *t*-test.

*Angiogenesis Assays.* The angiogenic activity of wild-type ANG and selected variants was measured by a thoracic aorta assay (*22*, *40*). Aortas were isolated from 6−8-week-old MF1 female mice, cleaned, and flushed with MCDB131 medium (Invitrogen) containing 100 units mL$^{-1}$ penicillin and 100 $\mu$g mL$^{-1}$ streptomycin (Sigma). Prior to use, growth factor-reduced (GFR) Matrigel (Becton Dickinson) was diluted 1:1 with a low-serum medium [consisting of MCDB131 supplemented with 0.1% murine serum (MS) (Autogen Bioclear), 100 units mL$^{-1}$ penicillin, 100 $\mu$g mL$^{-1}$ streptomycin, 2 mM L-glutamine, and 25 mM $NaHCO_3$] and kept on ice. Cross-sectional slices of aorta were placed in 50 $\mu$L of GFR Matrigel in wells of 48-well plates and incubated for 30 min to allow the Matrigel to set. Low-serum MCDB131 medium with or without test protein (200 ng mL$^{-1}$ ANG or ANG variant) was then added to each well. Incubation was continued for 5 days, during which time daily observations were made and the number of cellular processes per aortic section was recorded. The results of two experiments, each with four aorta slices per test sample, were combined. Test samples and negative controls (medium with 0.1% mouse serum) were tested on slices from the same aorta to minimize the biological variation between mice. All data were analyzed by Student's paired *t*-test.

*Circular Dichroic Spectroscopy and Thermal Unfolding Studies.* Circular dichroism (CD) studies were performed on a Jasco J-600 spectropolarimeter with a 2-mm rectangular cell. Samples of wild-type ANG and Q12L, K17E, K17I, R31K, C39W, K40I, and I46V variants were dissolved at a concentration of 0.1 mg/mL in 20 mM sodium acetate (pH 6.0) containing 0.1 M sodium chloride. Wavelength scans were performed at 20 °C from 195 to 250 nm at a rate of 50 nm/min. For thermal unfolding studies, ellipticity was continuously monitored at 220 nm while the temperature was raised by use of a Jasco PFD-425S temperature control unit from 20 to 80 °C at a rate of 50 °C/h.

Reversibility of thermal unfolding was checked by determining the CD spectrum (195−250 nm) after cooling to room temperature. To determine the midpoint of the unfolding transition ($T_m$) and $\Delta H$ of unfolding, baselines for changes in ellipticity of the folded and unfolded states were determined by linear regression analysis of data below and above the thermal transition and used to calculate the fraction of folded and unfolded protein at each data point. These values were then analyzed by fitting into equations for determining the $T_m$ and enthalpy of folding from changes in ellipticity as a function of temperature (eq 1) (http://www2.umdnj.edu/cdrwjweb/ thermody.txt), where *u* is the ellipticity of 100% folded protein, *l* is the ellipticity of unfolded protein, *h* is enthalpy, *t* is temperature, $t_m$ is temperature of melting, and $\theta$ is calculated ellipticity. This treatment assumes that the heat capacities for the folded and unfolded states are equal.

$$\theta = (u - l)\frac{\exp\left[\frac{h}{1.987t}\left(\frac{t}{t_m} - 1\right)\right]}{1 + \exp\left[\frac{h}{1.987t}\left(\frac{t}{t_m} - 1\right)\right]} + l \qquad (1)$$

The enthalpy of unfolding at $T_m$ was used to calculate the entropy of unfolding from the relationship: $\Delta S_m = \Delta H_m / T_m$, and the effects of mutations on stability at the $T_m$ of the mutant protein ($\Delta\Delta G_T$) were calculated from changes in $T_m$ from the relationship

$$\Delta\Delta G_T = \Delta H_{Tm}(1 - T/T_m) - \Delta C_p\{(T_m - T) + T \ln (T/T_m)\}$$

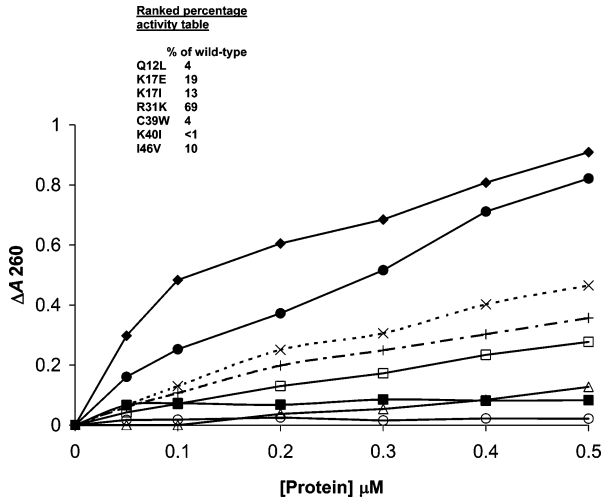


FIGURE 2: Ribonucleolytic activities of ANG (◆) and of Q12L (■), K17I (+), K17E (×), R31K (●), C39W (△), K40I (○), and I46V (□) variants toward tRNA. Assays measure the production of perchloric acid-soluble fragments (see Experimental Procedures). $\Delta A_{260}$ is the difference between the $A_{260}$ values measured in the presence and absence of test sample. Each data point represents the mean of three measurements. In all cases, the standard deviation is less than 2% of the mean. The activities listed on the figure are the means of the values calculated for 0.3, 0.4, and 0.5 $\mu$M variant.

where $T$ is the midpoint of unfolding for the mutant protein and $T_m$ is the midpoint of unfolding of the wild-type protein (both in kelvins), $\Delta H_{Tm}$ is the enthalpy of unfolding at $T_m$ (wild-type), and $\Delta C_p$ is the heat capacity change for unfolding. In the absence of a value for $\Delta C_p$ for ANG, we used a value of 1.15 kcal mol$^{-1}$ K$^{-1}$ reported by Pace et al. (*41*) for ribonuclease A.

*Molecular Modeling Studies.* The ALS mutations were modeled using the crystal structure of ANG at 1.8 Å resolution (PDB code 1B1I; *32*). Individual mutations were introduced into the structure by use of the graphics program COOT (*42*). All the mutated models were then subjected to 200 steps of conjugate gradient minimization by the program CNS (*43*). This was followed by an annealing schedule with a starting molecular dynamics temperature of 298 K. The locations of the mutated residues in the ANG structure are shown in Figure 1.

## RESULTS

*Ribonucleolytic Activity of ANG Variants.* The effects of the seven ALS-associated mutations on the ribonucleolytic potency of ANG were assessed with yeast tRNA as substrate (Figure 2). All of the variants except for R31K had substantially lower activity than wild-type ANG, ranging from 19% (K17E) to less than 1% (K40I). For R31K, the shape of the activity profile differs markedly from that with wild type, and the level of activity thus depends strongly on which portion of the curve is used: for example, R31K activity measured at 0.1 $\mu$M is 42% of that for wild ype, whereas at 0.5 $\mu$M it is 83%.

*Circular Dichroic Spectra and Thermal Unfolding of ANG Variants.* The effects of the mutations on folding and stability were assessed by CD spectroscopy. The far-UV CD spectra of the variants were generally similar to that of wild-type ANG, suggesting that the mutations have not significantly affected the secondary structure (Figure 3A). The $T_m$ for thermal unfolding, followed by measuring ellipticity at 220 nm as a function of temperature (Figure 3B, Table 2), was markedly decreased for the C39W variant, from 63.39 to 43.85 °C ($\Delta\Delta G = -4.51$ kcal/mol). Consequently, this variant is partially unfolded at physiological temperatures. The K40I and I46V variants showed moderate decreases in $T_m$ (5.29 and 6.22 °C, respectively), whereas the $T_m$ values for the other four variants were more similar to that of wild-type ANG.

*Effects of ANG Variants on the Established Biological Activities of ANG.* We investigated the effects of the Q12L, C39W, and K40I variants on the proliferation and angiogenic activity of ANG (*22*). These three variants were selected because they showed strongest reductions in ribonucleolytic activity. Their ability to induce angiogenesis was assayed by the thoracic aorta assay. This assay offers distinct advantages over the chick embryo chorioallantoic membrane assay used in most previous studies on ANG: most importantly, it provides a quantitative readout and utilizes a mammalian system.

In the thoracic aorta assay, no cellular processes were formed in the absence of test sample, and the addition of wild-type ANG caused by far the largest amount of angiogenic sprouting, with an average of 16 cellular processes per aorta on day 5 ($p < 0.002$ vs negative control, $n = 8$). The Q12L variant showed low angiogenic activity with an average of 7 cellular processes per aortic section on day 5 ($p < 0.02$ vs negative control, $n = 8$). The C39W and K40I variants showed a marginal increase in sprouting over the negative control with an average of 2 cellular processes per aortic section when compared with the negative control ($p < 0.02$ and $p < 0.04$, respectively, on day 5). The activities of all three were significantly lower than that of wild-type ANG ($p < 0.024$, $p < 0.003$, and $p < 0.001$ for Q12L, C39W, and K40I, respectively; $n = 8$) (Figure 4).

The addition of wild-type ANG to IGR1 cells caused an increase in proliferation over a period of 4 days that was significantly above that seen in 0.1% FCS medium alone on day 4 ($p < 0.0001$, $n = 10$). Proliferation of IGR1 was affected to varying degrees upon treatment with the variants Q12L, C39W, and K40I. The Q12L variant caused a small increase in cell proliferation above that seen in 0.1% FCS medium over the same period, which was significant at day 4 ($p < 0.001$, $n = 10$), whereas C39W and K40I were not significantly active compared to the negative control ($p = 0.42$ and 0.06, respectively). Cell proliferation in the presence of the C39W and K40I variants was lower than that seen with the wild-type ANG protein ($p < 0.001$, $n = 10$ in both cases) (Figure 5).

*Molecular Modeling of the ANG Variant Structures.* The seven variants were modeled to investigate the structural bases for the functional effects of the mutations. In the Q12L, R31K, and K40I models, there were no significant differences compared to wild-type ANG beyond the replacement itself. In all three, the new residue is shorter than the original amino acid but otherwise occupies the same position. Residues 12 and 40 are in the active-site region, and the substitutions eliminate side-chain hydrogen bonds while leaving many of the van der Waals contacts intact. Residue 31 is on the surface far from the catalytic site, and the Lys residue in the model is able to form most of the same interactions as the original Arg.

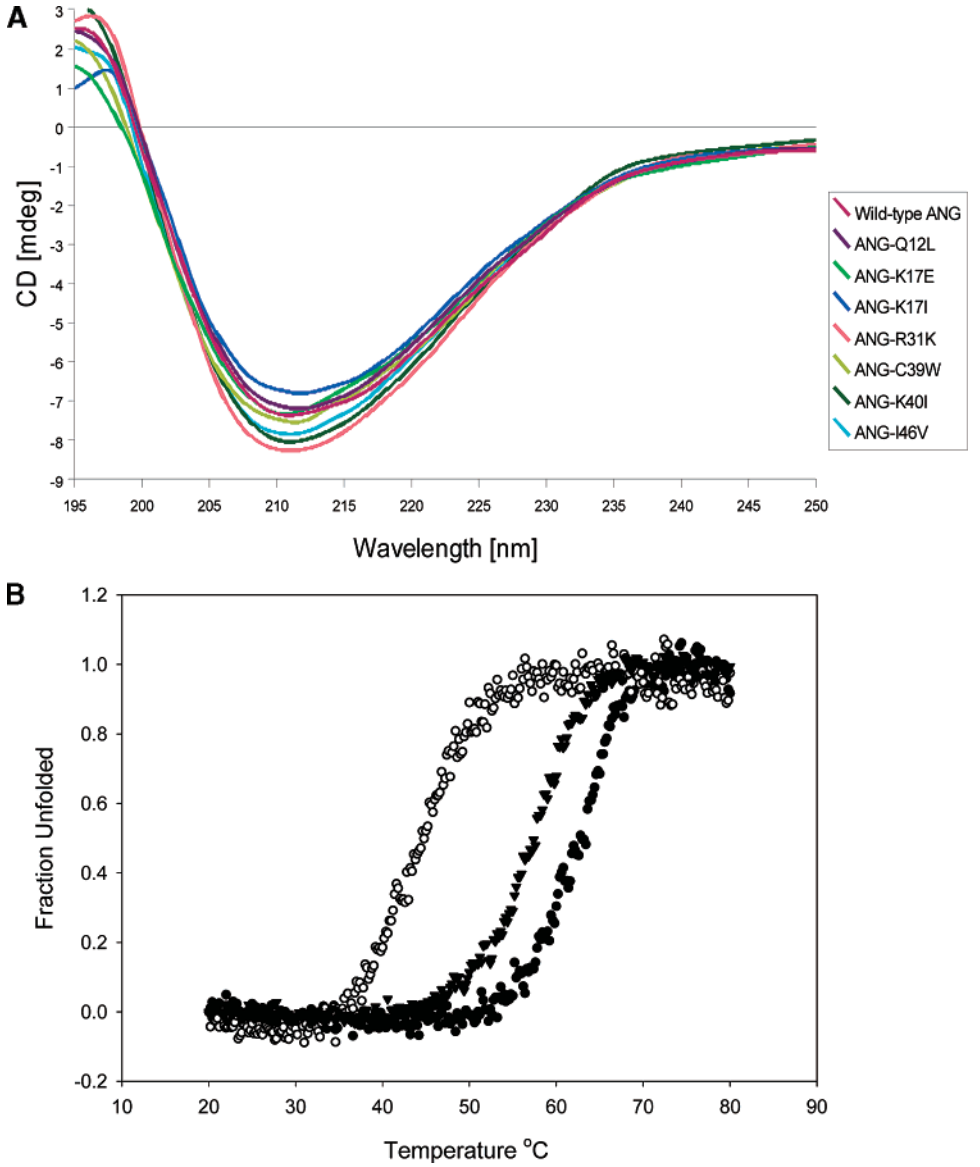


FIGURE 3: (A) CD spectral analysis for wild-type ANG and variants performed at 20 °C. Samples of wild-type ANG and Q12L, K17E, K17I, R31K, C39W, K40I, and I46V mutants were dissolved at a concentration of 0.1 mg/mL in 20 mM sodium acetate (pH 6.0) containing 0.1 M sodium chloride. Wavelength scans were performed at 20 °C from 195 to 250 nm at a scan rate of 50 nm/min. (B) Thermal unfolding of ANG and selected variants. The graph shows fraction unfolded, determined by circular dichroism at different temperatures. (●) Wild-type ANG; (○) C39W variant; (▼) I46V variant.

Table 2: Thermal Stability Results for ANG Variants

| protein | $T_m$ (°C) | $\Delta H_{Tm}$ (kcal mol$^{-1}$) | $\Delta S_m$ (kcal mol$^{-1}$ K$^{-1}$) | $\Delta\Delta G$ (kcal mol$^{-1}$) |
|---|---|---|---|---|
| ANG (native) | 63.39 ± 0.07 | −77.89 ± 1.55 | −0.231 ± 0.005 | 0 |
| Q12L | 62.30 ± 0.07 | −78.98 ± 1.64 | −0.235 ± 0.005 | −0.25 |
| K17E | 64.02 ± 0.08 | −79.36 ± 2.03 | −0.235 ± 0.006 | 0.15 |
| K17I | 61.37 ± 0.07 | −65.28 ± 1.61 | −0.195 ± 0.005 | −0.48 |
| R31K | 61.36 ± 0.09 | −82.43 ± 2.48 | −0.246 ± 0.007 | −0.48 |
| C39W | 43.85 ± 0.08 | −59.99 ± 1.28 | −0.189 ± 0.004 | −5.19 |
| K40I | 58.10 ± 0.05 | −69.02 ± 0.97 | −0.208 ± 0.003 | −1.27 |
| I46V | 57.17 ± 0.05 | −68.62 ± 0.92 | −0.207 ± 0.002 | −1.50 |

In the remaining four models, some structural perturbations are observed, although none appear to affect the active site. The most dramatic changes are in C39W, where the new Trp residue inserts into the hydrophobic core, essentially where the 39−92 disulfide is positioned in wild-type ANG. Consequently, Thr36 and Cys92 are displaced considerably: by 3.2 and 4.3 Å for the side-chain atoms OH and SH, respectively, and by 1.5−2.0 Å for the Cα atoms. For the two K17 variants, there is a ~1 Å shift in the backbone of the loop carrying the mutated residue but the positions of the substituted side chains (Glu/Ile) are similar to that of the original Lys. In the I46V model there is a small shift in the main chain of V46 that allows the side chain to fill in somewhat the space left by the removal of the δ methyl group.

## DISCUSSION

We have characterized the ALS-associated variants with regard to the enzymatic and biological properties of ANG as a starting point toward understanding the role of the

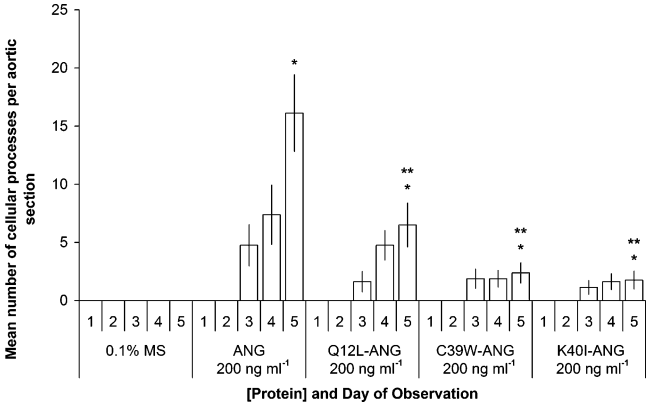


FIGURE 4: Angiogenic activities of ANG and Q12L, C39W, and K40I variants as determined by thoracic aorta assay. Histograms show the mean number (±SE; $n = 8$) of cellular processes growing from thoracic aorta sections on days 1−5 in the presence of 0.1% MS alone (negative control) or 0.1% MS plus 200 ng mL$^{-1}$ of the indicated protein. Assays were performed as reported in Crabtree et al. (*22*). A single asterisk denotes values significantly above that of the negative control on day 5. A double asterisk denotes values significantly below that seen in the ANG sample on day 5. Significance was tested by Student's paired *t*-test.

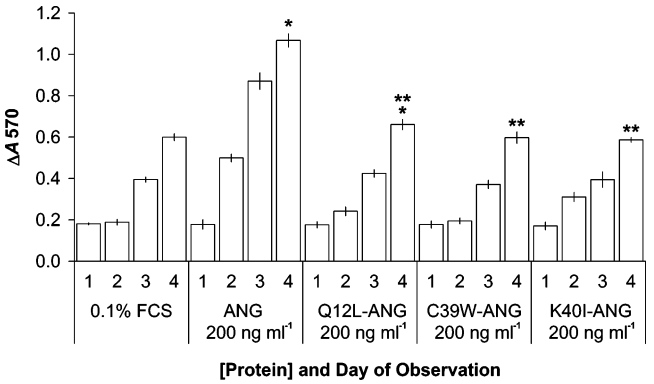


FIGURE 5: Proliferative activities of ANG and Q12L, C39W, and K40I variants. Histograms show proliferation of IGR1 cells in the presence and absence of ANG and ANG variants, as determined by MTT assay. The negative control was 0.1% FCS. Angiogenins were assayed at 200 ng mL$^{-1}$ in the presence of 0.1% FCS. Assays were performed as reported in Crabtree et al. (*22*). Error bars indicate standard deviations ($n = 10$). Single asterisks denote values significantly above the negative control on day 4. Double asterisks denote values significantly below the wild-type ANG samples on day 4.

mutations in the disease. We find that all of the variants with the exception of R31K have strongly reduced RNase activity (Figure 2). On the basis of CD measurements, all the variants are correctly folded and have not undergone any extensive changes in secondary structure (Figure 3A). However, the thermal stability of some of the variants is lower than that of wild-type ANG (Table 2, Figure 3B). The reductions in the ribonucleolytic potency of Q12L, C39W, and K40I are paralleled by marked decreases in angiogenic and mitogenic activity (Figures 4 and 5).

Mutation of Lys40 to Ile abolished all detectable RNase activity. Lys40 has been shown previously to be a key catalytic residue (*19*): replacement by Gln or a conservative substitution by Arg lowers RNase activity by >2000-fold and 50-fold, respectively. It is likely that the role of Lys40 is to stabilize the transition state during RNA cleavage, as for Lys41 in RNase A (*44*).

The variant C39W also has very low ribonucleolytic activity. This mutation eliminates a disulfide bridge with Cys92 that is conserved throughout the pancreatic RNase superfamily. Removal of the corresponding disulfide bond in RNase A decreases enzymatic activity by 11-fold (Ala mutations) or 20-fold (Ser mutations) and lowers $T_m$ by 21.8 °C (Ala mutations), similar to the present findings for C39W-ANG (*45*). In addition, our modeling study predicts that the new Trp residue in C39W might cause perturbations that have an effect on catalytic activity beyond that due to simple loss of the stabilizing disulfide.

Crystal structures of ANG show that Gln12 forms part of the $P_1$ subsite where phosphodiester bond cleavage occurs; it makes hydrogen bonds with Lys40 (*32*) and, in the complex of ANG with phosphate, with ligand as well (*46*). However, previous studies on this residue (*47*) and on its counterpart Gln11 in RNase A (*48*) have shown that replacement by Ala does not cause any significant loss of activity, which therefore indicates that Gln12/Gln11 is not a critical residue. Thus the considerable loss of RNase activity that we observe for the ANG-Q12L variant could be due to a specific deleterious effect of the Leu residue: placement of a hydrophobic residue in a hydrophilic active site that is set up to bind a phosphate group might have a disruptive effect.

Lys17 is conserved in ANG from cow, pig, rabbit, mouse, and several non-human primate species, but is replaced by Arg in one non-human primate and by Thr in six others. The residue lies on a surface loop distant from the catalytic site, and it is unlikely that substitution by Ile or Glu would have any dramatic effect on the structure. In keeping with this, these mutations have relatively minor effects on thermal stability and the model structures are quite similar to that of wild-type ANG. Nonetheless, our results show substantial (5−8-fold) activity losses for K17I and K17E. A previous study (*49*) demonstrated that replacement of ANG residues 8−22 by RNase A residues 7−21 (thus replacing Lys17 by a Ser, along with many other changes) markedly decreases the potency of ANG in inhibiting cell-free protein synthesis, an activity that has been attributed to the action of ANG on rRNA in intact ribosomes (*50*). Lys17 may be part of a peripheral recognition site for rRNA, and since the natural substrate of ANG is not yet known, it is possible that Lys17 is also involved in binding this substrate.

The relatively minor effect of the Arg31 to Lys mutation is consistent with earlier results showing that R31A is 92% as active as wild-type ANG (*51*). Although Arg31 is not involved in enzymatic activity, it is part of a nuclear translocation sequence, $^{31}$RRRGL$^{35}$, that is essential for angiogenic activity (*23*, *24*). R31A is translocated less efficiently than the native protein (*23*), and it is somewhat less effective than wild-type ANG at inducing angiogenesis (*51*). In the native structure Arg31 is involved in interactions with other residues but is largely accessible to the solvent (*32*). While it is possible that R31K is deficient in nuclear translocation, it should be noted that both Lys and Arg can function in nuclear translocation sequences (*52*). Moreover, bovine, pig, rabbit, and mouse ANG contain Lys rather than Arg at this position, and all are angiogenic (*53*, *54*). Thus, if the involvement of the R31K mutation with ALS reflects

loss of function, this function would most likely be one for which structure−function relationships have not yet been established in detail.

The I46V mutation results in a 10-fold decrease in RNase activity. The large magnitude of this change was surprising because Ile46 is not in the active site, and the loss of a single methyl group from its side chain might be expected to have only a minor effect on the structure (as predicted in the model). However, Ile46 lies within the hydrophobic core of the protein (*32*), where it is surrounded by several other hydrophobic residues. Interestingly, rabbit ANG and RNase A also have a Val residue at this position. However, in these proteins there are compensating changes in adjacent residues: Ile for Val at position 103 and Phe in place of Leu115 (human ANG numbering). Consequently, side-chain packing in the core may not be affected as greatly in these other enzymes by the Ile to Val change at position 46. The thermal stability of the I46V variant is significantly reduced compared to that of wild-type ANG, and the structural perturbation indicated by this decrease might also affect the functioning of the active site.

It is interesting to note that two of the ANG variants (C39W and I46V, both with significant destabilization) are associated with a familial history of ALS with early onset (*12*).

## CONCLUSION

Our results show that six of the seven ALS-linked mutations markedly diminish the ribonucleolytic activity of ANG and suggest that reduction of enzymatic potency may underlie the association of these mutations with the disease. Some of these mutations (K40I and Q12L) clearly have a direct impact on the catalytic center, whereas the others may affect activity indirectly (C39W, I46V) or by damaging a peripheral substrate binding site (K17I, K17E). Where indirect effects are involved, these may be mediated in part by decreases in stability. The three variants with the lowest enzymatic activity (K40I, Q12L, and C39W) were also characterized with respect to angiogenic and mitogenic activity and found to be much less active than wild-type ANG. In the one case (R31K) where the ALS-linked mutation has no appreciable effect on enzymatic activity, our results do not suggest any explanation for the disease association, and further studies will be required.

It is as yet unclear whether the molecular events underlying the angiogenic activity and the normal mechanism of action of ANG in the nervous system are similar and how these are perturbed in the hANG-ALS variants. Our study suggests that the mechanisms are likely to be similar. This is not surprising since molecules involved in vasculogenesis and angiogenesis such as VEGF have also been shown to play important roles in the nervous system (*8*, *10*, *55*).

It should be noted that ANG action involves cellular uptake, and at some point the ANG molecule is located in the cytosol. It is possible that the decreased stability and predicted alterations in structure could make the protein a target of ubiquitination and degradation by the proteasome, producing a major disruption in function. Alternatively, some mutations may affect the recognition of in vivo RNA targets. Further biological experiments with the ALS-implicated variants might provide some of the answers for the questions posed here.

## ACKNOWLEDGMENT

We thank Paul Veazey for his contribution during the early stages of the work.

## REFERENCES

1. Bruijn, L. I., Miller, T. M., and Cleveland, D. W. (2004) Unraveling the mechanisms involved in motor neuron degeneration in ALS, *Annu. Rev. Neurosci. 27*, 723−749.
2. Boillée, S., Velde, C. V., and Cleveland, D. W. (2006) ALS: a disease of motor neurons and their non-neuronal neighbors, *Neuron 52*, 39−59.
3. Rosen, D. R., Siddique, T., Patterson, D., Figlewicz, D. A., Sapp, P., Hentati, A., Donaldson, D., Goto, J., O'Regan, J. P., Deng, H. X., Rahmani, Z., Krizus, A., McKenna-Yasek, D., Cayabyab, A., Gaston, S. M., Berger, R., Tanzi, R. E., Halperin, J. J., Herzfeldt, B., van den Bergh, R., Hung, W.-y., Bird, T., Deng, G., Mulder, D. M., Smyth, C., Laing, N. G, Soriano, E., Pericak-Vance, M. A., Haines, J., Rouleau, G. A., Gusella, J. S., Horvitz, H. R., and Brown, R. H., Jr. (1993) Mutations in Cu/Zn superoxide dismutase gene are associated with familial amyotrophic lateral sclerosis, *Nature 362*, 59−62.
4. Nishimura, A. L., Mitne-Neto, M., Silva, H. C., Richieri-Costa, A., Middleton, S., Cascio, D., Kok, F., Oliveira, J. R., Gillingwater, T., Webb, J., Skehel, P., and Zatz, M. (2004) A mutation in the vesicle-trafficking protein VAPB causes late-onset spinal muscular atrophy and amyotrophic lateral sclerosis, *Am. J. Hum. Genet. 75*, 822−831.
5. Yang, Y., Hentati, A., Deng, H. X., Dabbagh, O., Sasaki, T., Hirano, M., Hung, W. Y., Ouahchi, K., Yan, J., Azim, A. C., Cole, N., Gascon, G., Yagmour, A., Ben-Hamida, M., Pericak-Vance, M., Hentati, F., and Siddique, T. (2001) The gene encoding alsin, a protein with three guanine-nucleotide exchange factor domains, is mutated in a form of recessive amyotrophic lateral sclerosis, *Nat. Genet. 29*, 160−165.
6. Chen, Y. Z., Bennett, C. L., Huynh, H. M., Blair, I. P., Puls, I., Irobi, J., Dierick, I., Abel, A., Kennerson, M. L., Rabin, B. A., Nicholson, G. A., Auer-Grumbach, M., Wagner, K., De Jonghe, P., Griffin, J. W., Fischbeck, K. H., Timmerman, V., Cornblath, D. R., and Chance, P. F. (2004) DNA/RNA helicase gene mutations in a form of juvenile amyotrophic lateral sclerosis (ALS4), *Am. J. Hum. Genet. 74*, 1128−1135.
7. Oosthuyse, B., Moons, L., Storkebaum, E., Beck, H., Nuyens, D., Brusselmans, K., van Dorpe, J., Hellings, P., Gorselink, M., Heymans, S., Theilmeier, G., Dewerchin, M., Laudenbach, V., Vermylen, P., Raat, H., Acker, T., Vleminckx, V., van Den Bosch, L., Cashman, N., Fujisawa, H., Drost, M. R., Sciot, R., Bruyninckx, F., Hicklin, D. J., Ince, C., Gressens, P., Lupu, F., Plate, K. H., Robberecht, W., Herbert, J. M., Collen, D., and Carmeliet, P. (2001) Deletion of the hypoxia-response element in the vascular endothelial growth factor promoter causes motor neuron degeneration, *Nat. Genet. 28*, 131−138.
8. Lambrechts, D., Storkebaum, E., Morimoto, M., Del-Favero, J., Desmet, F., Marklund, S. L., Wyns, S., Thijs, V., Andersson, J., van Marion, I., Al-Chalabi, A., Bornes, S., Musson, R., Hansen, V., Beckman, L., Adolfsson, R., Pall, H. S., Prats, H., Vermeire, S., Rutgeerts, P., Katayama, S., Awata, T., Leigh, N., Lang-Lazdunski, L., Dewerchin, M., Shaw, C., Moons, L., Vlietinck, R., Morrison, K. E., Robberecht, W., van Broeckhoven, C., Collen. D., Andersen, P. M., and Carmeliet, P. (2003) VEGF is a modifier of amyotrophic lateral sclerosis in mice and humans and protects motoneurons against ischemic death, *Nat. Genet. 34*, 383−394.
9. Lambrechts, D., Lafuste, P., Carmeliet, P., and Conway, E. M. (2006) Another angiogenic gene linked to amyotrophic lateral sclerosis, *Trends Mol. Med. 12*, 345−347.
10. Storkebaum, E., Lambrechts, D., Dewerchin, M., Moreno-Murciano, M. P., Appelmans, S., Oh, H., van Damme, P., Rutten, B., Man, W. Y., de Mol, M., Wyns, S., Manka, D., Vermeulen, K., van Den, Bosch, L., Mertens, N., Schmitz, C., Robberecht, W., Conway, E. M., Collen, D., Moons, L., and Carmeliet, P. (2005) Treatment of motoneuron degeneration by intracerebroventricular delivery of VEGF in a rat model of ALS, *Nat. Neurosci. 8*, 85−92.

11. Greenway, M. J., Alexander, M. D., Ennis, S., Traynor, B. J., Corr, B., Frost, E., Green, A., and Hardiman, O. (2004) A novel candidate region for ALS on chromosome 14q11.2, *Neurology 63*, 1936−1938.
12. Greenway, M. J., Andersen, P. M., Russ, C., Ennis, S., Cashman, S., Donaghy, C., Paterson, V., Swingler, R., Morrison, K. E., Green, A., Acharya, K. R., Brown, R. H., Jr., and Hardiman, O. (2006) Loss-of-function *ANG* mutations segregate with familial and 'sporadic' amyotrophic lateral sclerosis, *Nat. Genet. 38*, 411−413.
13. Subramanian, V., and Feng, Y. (2007) A new role for angiogenin in neurite growth and pathfinding—implications for amyotrophic lateral sclerosis, *Hum. Mol. Genet. 16*, 1445−1453.
14. Fett, J. W., Strydom, D. J., Lobb, R. R., Alderman, E. M., Bethune, J. L., Riordan, J. F., and Vallee, B. L. (1985) Isolation and characterization of angiogenin, an angiogenic protein from human carcinoma cells, *Biochemistry 24*, 5480−5486.
15. Adams, S. A., and Subramanian, V. (1999) The angiogenins: an emerging family of ribonuclease related proteins with diverse cellular functions, *Angiogenesis 3*, 189−199.
16. Riordan, J. F. (2001) Angiogenin, *Methods Enzymol. 341*, 263−273.
17. Shapiro, R., Riordan, J. F., and Vallee, B. L. (1986) Characteristic ribonucleolytic activity of human angiogenin, *Biochemistry 25*, 3527−3532.
18. Harper, J. W., and Vallee, B. L. (1989) A covalent angiogenin/ribonuclease hybrid with a fourth disulfide bond generated by regional mutagenesis, *Biochemistry 28*, 1875−1884.
19. Shapiro, R., Fox, E. A., and Riordan, J. F. (1989) Role of lysines in human angiogenin: chemical modification and site-directed mutagenesis, *Biochemistry 28*, 1726−1732.
20. Shapiro, R., and Vallee, B. L. (1989) Site-directed mutagenesis of histidine-13 and histidine-114 of human angiogenin. Alanine derivatives inhibit angiogenin-induced angiogenesis, *Biochemistry 28*, 7401−7408.
21. Curran, T. P., Shapiro, R., and Riordan, J. F. (1993) Alteration of the enzymatic activity of human angiogenin by site-directed mutagenesis, *Biochemistry 32*, 2307−2313.
22. Crabtree, B., Holloway, D. E., Baker, M. D., Acharya, K. R., and Subramanian, V. (2007) Biological and structural features of murine angiogenin-4, an angiogenic protein, *Biochemistry 46*, 2431−2443.
23. Moroianu, J., and Riordan, J. F. (1994) Identification of the nuclear targeting signal of human angiogenin, *Biochem. Biophys. Res. Commun. 203*, 1765−1772.
24. Moroianu, J., and Riordan, J. F. (1994) Nuclear translocation of angiogenin in proliferating endothelial cells is essential to its angiogenic activity, *Proc. Natl. Acad. Sci. U.S.A. 91*, 1677−1681.
25. Badet, J., Soncin, F., Guitton, J. D., Lamare, O., Cartwright, T., and Barritault, D. (1989) Specific binding of angiogenin to calf pulmonary artery endothelial cells, *Proc. Natl. Acad. Sci. U.S.A. 86*, 8427−8431.
26. Hu, G. F., Riordan, J. F., and Vallee, B. L. (1997) A putative angiogenin receptor in angiogenin-responsive human endothelial cells, *Proc. Natl. Acad. Sci. U.S.A. 94*, 2204−2209.
27. Hu, G. F., Riordan, J. F., and Vallee, B. L. (1994) Angiogenin promotes invasiveness of cultured endothelial cells by stimulation of cell-associated proteolytic activities, *Proc. Natl. Acad. Sci. U.S.A. 91*, 12096−12100.
28. Jimi, S., Ito, K., Kohno, K., Kuwano, M., Itagaki, Y., and Ishikawa, H. (1995) Modulation by bovine angiogenin of tubular morphogenesis and expression of plasminogen activator in bovine endothelial cells, *Biochem. Biophys. Res. Commun. 211*, 476−483.
29. Hartmann, A., Kunz, M., Kostlin, S., Gillitzer, R., Toksoy, A., Brocker, E. B., and Klein, C. E. (1999) Hypoxia-induced up-regulation of angiogenin in human malignant melanoma, *Cancer Res. 59*, 1578−1583.
30. Nakamura, M., Yamabe, H., Osawa, H., Nakamura, N., Shimada, M., Kumasaka, R., Murakami, R., Fujita, T., Osanai, T., and Okumura, K. (2006) Hypoxic conditions stimulate the production of angiogenin and vascular endothelial growth factor by human renal proximal tubular epithelial cells in culture, *Nephrol., Dial., Transplant. 21*, 1489−1495.
31. Acharya, K. R., Shapiro, R., Allen, S. C., Riordan, J. F., and Vallee, B. L. (1994) Crystal structure of human angiogenin reveals the structural basis for its functional divergence from ribonuclease, *Proc. Natl. Acad. Sci. U.S.A. 91*, 2915−2919.
32. Leonidas, D. D., Shapiro, R., Allen, S. C., Subbarao, G. V., Veluraja, K., and Acharya, K. R. (1999) Refined crystal structures of native human angiogenin and two active site variants: implications for the unique functional properties of an enzyme involved in neovascularisation during tumour growth, *J. Mol. Biol. 285*, 1209−1233.
33. Acharya, K. R., Shapiro, R., Riordan, J. F., and Vallee, B. L. (1994) Crystal structure of bovine angiogenin at 1.5Å resolution, *Proc. Natl. Acad. Sci. U.S.A. 92*, 2949−2953.
34. Holloway, D. E., Chavali, G. B., Hares, M. C., Subramanian, V., and Acharya K. R. (2005) Structure of murine angiogenin: features of the substrate- and cell-binding regions and prospects for inhibitor-binding studies, *Acta Crystallogr. D61*, 1568−1578.
35. Shapiro, R., Harper, J. W., Fox, E. A., Jansen, H. W., Hein, F., and Uhlmann, E. (1988) Expression of Met-(−1) angiogenin in *Escherichia coli*: conversion to the authentic <Glu-1 protein, *Anal. Biochem. 175*, 450−461.
36. Holloway, D. E., Hares, M. C., Shapiro, R., Subramanian, V., and Acharya, K. R. (2001) High-level expression of three members of the murine angiogenin family in *Escherichia coli* and purification of the recombinant proteins, *Protein Expression Purif. 22*, 307−317.
37. Shapiro, R., and Vallee, B. L. (1991) Interaction of human placental ribonuclease with placental ribonuclease inhibitor, *Biochemistry 30*, 2246−2255.
38. Pace, C. N., Vajdos, F., Fee, L., Grimsley, G., and Gray, T. (1995) How to measure and predict the molar absorption coefficient of a protein, *Protein Sci. 4*, 2411−2423.
39. Shapiro, R., Weremowicz, S., Riordan, J. F., and Vallee, B. L. (1987) Ribonucleolytic activity of angiogenin: essential histidine, lysine, and arginine residues, *Proc. Natl. Acad. Sci. U.S.A. 84*, 8783−8787.
40. Masson, V., Devy, L., Grignet-Debrus, C., Bernt, S., Bajou, K., Blacher, S., Roland, G., Chang, Y., Fong, T., Carmeliet, P., Foidart, J.-M., and Noël, A. (2002) Mouse aortic ring assay: a new approach of the molecular genetics of angiogenesis, *Biol. Proced. Online 4*, 24−31.
41. Pace, C. N., Grimsley, G. R., Thomas, S, T., and Makhatadze, G. I. (1999) Heat capacity change for ribonuclease A folding, *Protein Sci. 8*, 1500−1504.
42. Emsley, P., and Cowtan K. (2004) Coot: model-building tools for molecular graphics, *Acta Crystallogr. D60*, 2126−2132.
43. Brünger, A. T., Adams, P. D., Clore, G. M., Delano, W. M., Kuntleve, G. P., Jiang, J. S., Kuszewski, J., Nilges, M., Pannu, N. S., Read, R. J., Rice, L. M., Simonson, T., and Warren, G. L. (1998) Crystallography and NMR System: A new software suite for macromolecular structure determination, *Acta Crystallogr. D54*, 905−921.
44. Raines, R. T. (1998) Ribonuclease A, *Chem. Rev. 98*, 1045−1065.
45. Laity, J. H., Lester, C. C., Shimotakahara, S., Zimmerman, D. E., Montelione, G. T., and Scheraga, H. A. (1997) Structural characterization of an analog of the major rate-determining disulfide folding intermediate of bovine pancreatic ribonuclease A, *Biochemistry 36*, 12683−12699.
46. Leonidas, D. D., Chavali, G. B., Jardine, A. M., Li, S., Shapiro, R., and Acharya, K. R. (2001) Binding of phosphate and pyrophosphate ions at the active site of human angiogenin as revealed by X-ray crystallography, *Protein Sci. 10*, 1669−1676.
47. Jenkins, J. L., and Shapiro, R. (2003) Identification of small-molecule inhibitors of human angiogenin and characterization of their binding interactions guided by computational docking, *Biochemistry 42*, 6674−6687.
48. delCardayre, S. B., Ribo, M., Yokel, E. M., Quirk, D. J., Rutter, W. J., and Raines, R. T. (1995) Engineering ribonuclease A: production, purification and characterization of wild-type enzyme and mutants at Gln11, *Protein Eng. 8*, 261−273.
49. Bond, M. D., and Vallee, B. L. (1990) Replacement of residues 8−22 of angiogenin with 7−21 of RNase A selectivity affects protein synthesis inhibition and angiogenesis, *Biochemistry 29*, 3341−3349.
50. St. Clair, D. K., Rybak, S. M., Riordan, J. F., and Vallee, B. L. (1988) Angiogenin abolishes cell-free protein synthesis by specific ribonucleolytic inactivation of 40S ribosomes, *Biochemistry 27*, 7263−7268.
51. Shapiro, R., and Vallee, B. L. (1992) Identification of functional arginines of human angiogenin by site-directed mutagenesis, *Biochemistry 31*, 12477−12485.
52. Dingwall, C., and Laskey, R. A. (1991) Nuclear targeting sequences—a consensus? *Trends Biochem. Sci. 16*, 478−481.

53. Bond, M. D., Strydom, D. J., and Vallee, B. L. (1993) Characterization and sequencing of rabbit, pig and mouse angiogenins: discernment of functionally important residues and regions, *Biochim. Biophys. Acta 1162*, 177−186.
54. Nobile, V., Vallee, B. L., and Shapiro, R. (1996) Characterization of mouse angiogenin-related protein: implications for functional studies on angiogenin, *Proc. Natl. Acad. Sci. U.S.A. 93*, 4331−4335.
55. Suchting, S., Bicknell, R., and Eichmann, A. (2006) Neuronal clues to vascular guidance, *Exp. Cell Res. 312*, 668−675.

BI701333H